

Probabilistic Track Coverage in Cooperative Sensor Networks

Silvia Ferrari, *Senior Member, IEEE*, Guoxian Zhang, *Member, IEEE*, and Thomas A. Wettergren, *Senior Member, IEEE*

Abstract—The quality of service of a network performing cooperative track detection is represented by the probability of obtaining multiple elementary detections over time along a target track. Recently, two different lines of research, namely, distributed-search theory and geometric transversals, have been used in the literature for deriving the probability of track detection as a function of random and deterministic sensors' positions, respectively. In this paper, we prove that these two approaches are equivalent under the same problem formulation. Also, we present a new performance function that is derived by extending the geometric-transversal approach to the case of random sensors' positions using Poisson flats. As a result, a unified approach for addressing track detection in both deterministic and probabilistic sensor networks is obtained. The new performance function is validated through numerical simulations and is shown to bring about considerable computational savings for both deterministic and probabilistic sensor networks.

Index Terms—Geometric transversals, Poisson flats, probability, search theory, sensor networks, target tracking, track coverage, track detection.

I. INTRODUCTION

THE PROBLEM of track detection by cooperative sensor networks arises in many applications, including security and surveillance, environmental and atmospheric monitoring, and tracking of endangered species. The performance of these networks can be characterized by their area and track coverage, both of which have received considerable attention in the literature [1]–[10]. *Area coverage* is defined as the union of the areas representing the sensors' fields of view (FOVs), divided by the area of the region of interest (ROI) [3]–[5]. Area coverage is related to the probability of obtaining single independent target detections in the ROI [5]. *Track coverage* is defined as a Lebesgue measure of the tracks that intersect multiple FOVs, divided by the measure of all possible tracks through the ROI [8]. As shown in [8], track coverage is related to the probability of cooperatively detecting target tracks over time. A track is said to be detected when it can be formed

from multiple independent sensor detections using an assumed prior spatiotemporal model. Multiple independent detections are required by cost-effective sensors that have limited detection capabilities, and are subject to frequent false alarms. As in previous formulations [1]–[10], in this paper, we consider passive targets (e.g., aircraft and underwater vehicles) that can be assumed to move at constant speed and heading throughout a fixed ROI.

The probability of track detection of a uniformly distributed sensor network with constant detection ranges was first obtained in [11], [12] by modeling the moving target as a two-state Markov process. This approach, however, is not applicable to sensor networks that are not uniformly distributed, such as networks in which sensors' positions are optimized or are a function of time. Early studies in search theory obtained the probability that a single platform will detect a moving target at any time during a fixed and finite time horizon [13]–[16]. More recently, with the advent of wireless communication technologies, distributed-search theory has been successfully applied to cooperative sensor networks and has been used to derive the probability of track detection of a nonuniformly distributed sensor network [9]. The problem formulation in [9] assumes that the targets move at constant speed and heading through the ROI and that the sensors' positions and the track parameters are random and continuous in both space and time. Along a different line of research, the track coverage and the probability of track detection of a deterministic sensor network were derived in [8] using a geometric-transversal approach. The problem formulation in [8] assumes that the sensors' positions are deterministic and continuous in both space and time and that the target's speed and heading are uniformly distributed over their ranges.

The advantage of geometric transversals over other approaches is that the resulting performance metrics are trigonometric functions of the sensors' positions and detection ranges and can thus be optimized using sequential quadratic programming [8]. The advantage of the distributed-search approach is that it can account for random sensors' positions and for track parameters that are not uniformly distributed [9]. In this paper, we prove that the distributed-search approach presented in [9] and the geometric-transversal approach presented in [8] are equivalent under the same problem formulation and assumptions. A new function representing the probability of track detection is derived using Poisson flats, thereby extending the geometric-transversal approach in [8] to the case of random sensors' positions and nonuniform track parameters. As a result, a unified geometric-transversal approach is obtained for analyzing track detection in both deterministic and probabilistic sensor networks.

Manuscript received May 1, 2009; revised October 5, 2009; accepted December 17, 2009. Date of publication March 15, 2010; date of current version November 17, 2010. This work was supported in part by the Office of Naval Research under Code 321 and in part by the National Science Foundation under CAREER ECS 0448906. This paper was recommended by Associate Editor R. Lynch.

S. Ferrari and G. Zhang are with the Department of Mechanical Engineering and Materials Science, Duke University, Durham, NC 27708 USA (e-mail: sferrari@duke.edu).

T. A. Wettergren is with the Naval Undersea Warfare Center, Newport, RI 02841 USA (e-mail: t.a.wettergren@ieee.org).

Color versions of one or more of the figures in this paper are available online at <http://ieeexplore.ieee.org>.

Digital Object Identifier 10.1109/TSMCB.2010.2041449

This paper is organized as follows. The distributed-search and geometric-transversal approaches are reviewed in Section II. The problem formulation is described in Section III, and a function representing the probability of track detection is derived in Section IV. The analysis in Section V shows that the distributed-search and geometric-transversal approaches differ in the manner by which they construct the 3-D region of integration for the joint probability density function (pdf) of the sensors' positions and track parameters. The theoretical results are validated numerically in Section VI, demonstrating that the new probability function also brings about considerable computational savings.

II. BACKGROUND ON TRACK DETECTION

The problem of track detection is concerned with the probability that a target track is formed by a cooperative sensor network using elementary detections over time [12]. A track detection is declared at the data- or detection-report level when the track is formed from a minimum of k detections, in an approach known as track-before-detect [9]. By this approach, the tracks of targets that are unknown in number can be formed from data of multiple consecutive frames of observations using multiple-hypothesis tracking [17] or geometric invariants [2]. Track detection also provides a natural mechanism for providing tracking information concurrently with detection reports and for mitigating false alarms.

Then, the sensor network's performance can be represented by the *probability of track detection*, defined as the probability of obtaining k independent detections when one or more targets are present in the ROI. In [9], the probability of track detection was obtained for a nonuniform probabilistic sensor network using the theory of distributed search. Along a different line of research, the track coverage of a nonuniform deterministic sensor network was developed in [8] using geometric-transversal theory. In a deterministic network, the sensors' positions are viewed as vectors in Euclidean space, whereas in a probabilistic network, they are viewed as random variables sampled from a pdf. Typically, the deterministic view is well suited to networks of small to medium size, whose positions can be accurately determined or controlled. The probabilistic view, on the other hand, is well suited to large sensor networks and to networks that are subject to greater uncertainty.

This paper proves that the distributed-search and geometric-transversal approaches reviewed in the next sections are equivalent under the same problem formulation and assumptions, as described in Section III.

A. Review of Distributed-Search Approach

The distributed-search approach presented in [9] assumes that the sensors' positions and the target track's parameters are random variables and that the detection events may be modeled by a spatial Poisson process. Assume that a network of $n \geq k$ omnidirectional sensors is deployed in a square ROI, $\mathcal{A} \subset \mathbb{R}^2$, in order to track and detect moving targets. A sensor j positioned at $\mathbf{x}_j \in \mathcal{A}$ provides a detection report whenever a target at $\mathbf{x}_T \in \mathbb{R}^2$ comes within the sensor's detection range, r . The detection range is defined as the maximum range at which the received signal exceeds a desired threshold. All n sensors are assumed to have the same value of r and are represented

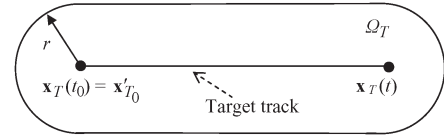


Fig. 1. Detection region for a straight target track over time interval $\Delta t = t - t_0$ (adapted from [9]).

by omnidirectional binary models. It follows that the FOV of the j th sensor can be represented by a circle $\mathcal{C}_j = \mathcal{C}(\mathbf{x}_j, r)$ that is centered at \mathbf{x}_j , and has a constant radius r . Furthermore, the j th sensor's probability of detection is equal to one everywhere in \mathcal{C}_j and is equal to zero elsewhere. The targets are assumed to move at constant speed V and heading θ and to maintain a constant source amplitude.

The distributed-search approach in [9] is based on the detection region $\Omega_T \subset \mathcal{A}$ that is grown isotropically from the target track

$$\mathbf{x}_T(t) = \mathbf{x}'_{T_0} + V(t - t_0)[\cos \theta \quad \sin \theta]^T \quad (1)$$

over a time interval Δt , where $t_0 \leq t \leq t_0 + \Delta t$, and $\mathbf{x}_T(t_0) = \mathbf{x}'_{T_0} \in \mathcal{A}$ is the target's initial position, as shown in Fig. 1. Then, the probability of track detection is obtained as a function of the pdf of the sensors' positions $f_{\mathbf{x}}(\mathbf{x}_j)$, the pdfs of the target speed $f_V(V)$, and heading $f_{\theta}(\theta)$, as well as the pdf of the initial position $f_T(\mathbf{x}'_{T_0})$. Let event $D_j = \{1, 0\}$ represent the set of all possible mutually exclusive outcomes corresponding to sensor j reporting (1) or not reporting (0) a target detection. Then, assuming that the targets are distributed uniformly in \mathcal{A} , the probability of a detection being reported by the j th sensor is given by a spatial Poisson process

$$\Pr \{D_j = 1 \mid \mathbf{x}_T(t) \in \mathcal{A}\} = 1 - e^{-\phi_t} \quad (2)$$

where

$$\phi_t(\mathbf{x}'_{T_0}, V, \theta) = \int_{\Omega_T(\mathbf{x}'_{T_0}, \theta, V \Delta t)} f_{\mathbf{x}}(\mathbf{x}_j) d\mathbf{x}_j \quad (3)$$

is the coverage factor of a sensor with a detection region Ω_T .

In a network of n sensors, the set of events $\{D_1, \dots, D_n\}$ is reported to a central processor, and a successful track detection is declared when $\sum_{j=1}^n D_j \geq k$. Then, the probability of a track detection by at least k sensors can be described using Bernoulli trials [18, Section 3.1]. It is assumed that the individual detection events are statistically identical and independent and that $\phi_t \ll 1$, and $n \gg 1$. Using the Poisson theorem and the Taylor series expansion of the exponential function, the probability of successful track detection in \mathcal{A} can be approximated by the integral function

$$\begin{aligned} P_t &= \Pr \left(\sum_{j=1}^n D_j \geq k \mid \mathbf{x}_T(t) \in \mathcal{A} \right) \\ &= 1 - \int_0^{2\pi} \int_{V_{\min}}^{V_{\max}} \int_{\mathcal{A}} e^{-n\phi_t(\mathbf{x}'_{T_0}, V, \theta)} f_T(\mathbf{x}'_{T_0}) \\ &\quad \times f_V(V) f_{\theta}(\theta) \sum_{m=0}^{k-1} \frac{[n\phi_t(\mathbf{x}'_{T_0}, V, \theta)]^m}{m!} d\mathbf{x}'_{T_0} dV d\theta \quad (4) \end{aligned}$$

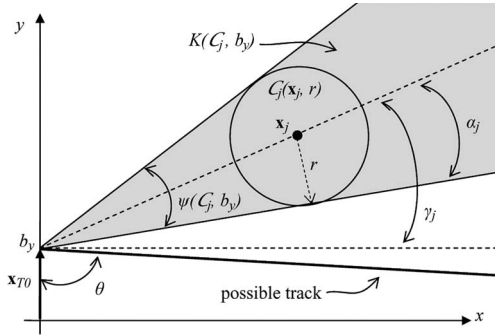


Fig. 2. Coverage cone of an omnidirectional sensor positioned at \mathbf{x}_j .

as shown in [9]. V_{\min} and V_{\max} are the target's minimum and maximum speeds, respectively, and function $\phi_t(\mathbf{x}'_{T_0}, V, \theta)$ is defined in (3). Using (4), the probability of track detection can be evaluated for different sensor distributions [9], and an approximately optimal sensor distribution can be determined in the form of a parameterized Gaussian mixture, as shown in [19].

An alternative performance function for cooperative track detection was developed in [8] using the geometric-transversal approach reviewed in the next section.

B. Review of Geometric-Transversal Approach

Geometric-transversal theory is concerned with the analysis of the space of transversals to a family of compact convex bodies in \mathbb{R}^d [20], [21]. A set of convex bodies in \mathbb{R}^d is said to have a j -transversal when the objects are simultaneously intersected by a j -dimensional flat, or translate, of a linear space. A line transversal ($j = 1$), referred to as *stabber*, with $d = 2$ and $k \geq 1$, is a straight line that intersects at least k members of a family of objects in \mathbb{R}^2 . When the target's heading θ remains constant in \mathcal{A} , its track can be represented by a 1-D flat in \mathbb{R}^2 . Therefore, a target track that is detected by k sensors at time $t \in \Delta t$ is a stabber of the family of n circles of radius r representing the detection circles of the sensors at t .

In [8], the geometric properties of circles and cones were used to construct efficient closed-form representations of sets of stabbers for families of circles representing omnidirectional sensors. These representations are based on the result that every set of stabbers of a detection circle \mathcal{C}_j is contained by a so-called *coverage cone* generated by \mathcal{C}_j and is measured by the cone's opening angle. Given a nonempty subset X of \mathbb{R}^n , the *cone generated by X* , denoted by $\text{cone}(X)$, is the set of all nonnegative combinations of the elements of X [22]. Place an inertial xy -frame along two sides \mathcal{A} , such that all target tracks traverse \mathcal{A} in the positive orthant \mathbb{R}_+^2 . Let $K(\mathcal{C}_j, b_y) = \text{cone}(\mathcal{C}_j)$ denote the coverage cone of the j th sensor, with origin at the y -intercept b_y , as shown in Fig. 2. Then, as proven in [8], the set of all tracks through b_y that are detected by the j th sensor are contained by coverage cone $K(\mathcal{C}_j, b_y)$, which is finitely generated by unit vectors

$$\hat{\mathbf{h}}_j = \begin{bmatrix} \cos \alpha_j & -\sin \alpha_j \\ \sin \alpha_j & \cos \alpha_j \end{bmatrix} \frac{\mathbf{v}_j}{\|\mathbf{v}_j\|} \equiv \mathbf{Q}^+(\alpha_j) \hat{\mathbf{v}}_j \quad (5)$$

$$\hat{\mathbf{l}}_j = \begin{bmatrix} \cos \alpha_j & \sin \alpha_j \\ -\sin \alpha_j & \cos \alpha_j \end{bmatrix} \frac{\mathbf{v}_j}{\|\mathbf{v}_j\|} \equiv \mathbf{Q}^-(\alpha_j) \hat{\mathbf{v}}_j \quad (6)$$

where $\mathbf{v}_j \equiv \mathbf{x}_j - \mathbf{x}_{T_0}$, $\mathbf{x}_{T_0} = [0 \ b_y]^T$, $\alpha_j = \sin^{-1}(r/\|\mathbf{v}_j\|)$, and $\|\cdot\|$ denotes the L_2 -norm. $\mathbf{Q}^+(\cdot)$ and $\mathbf{Q}^-(\cdot)$ denote the counterclockwise and clockwise rotation matrices, respectively, and (\cdot) denotes a unit vector. It follows that $K(\mathcal{C}_j, b_y)$ and its opening angle

$$\psi(\mathcal{C}_j, b_y) = 2\alpha_j = H\left(\|\hat{\mathbf{l}}_j \times \hat{\mathbf{h}}_j\|\right) \sin^{-1}\left(\|\hat{\mathbf{l}}_j \times \hat{\mathbf{h}}_j\|\right) \quad (7)$$

are functions of r and \mathbf{x}_j , with $H(\cdot)$ being the Heaviside function.

The unit vectors in (5) and (6) are also used to determine the k -coverage cones containing stabbers of k members in a family of n circles, $S = \{\mathcal{C}_1, \dots, \mathcal{C}_n\}$. As proven in [8], the set of stabbers through $y = b_y$ for a family of k circles $S_k = \{\mathcal{C}_1, \dots, \mathcal{C}_k\} \subset S$ is contained by a k -coverage cone $K_k(S_k, b_y)$ that is finitely generated by two unit vectors selected from the set $\{\hat{\mathbf{h}}_j, \hat{\mathbf{l}}_j \mid j = 1, \dots, n\}$ using linear operations. It was also shown in [8] that the opening angle of $K_k(S_k, b_y)$, denoted by $\psi(S_k, b_y)$, is a Lebesgue measure over the set of stabbers of S_k .

Place a second inertial $x'y'$ -frame of reference along the remaining two sides of \mathcal{A} . Then, Lebesgue measures on the stabbers with intercepts $x = b_x$, $y' = b_{y'}$, and $x' = b_{x'}$ can be obtained from the opening angles of the corresponding k -coverage cones, denoted by ζ , ξ , and ρ , respectively. The set of stabbers traversing \mathcal{A} and intersecting at least k members in S is approximated by the union of the k -coverage cones over a finite set of intercept values indexed by superscript ℓ . The intercept values are obtained by discretizing the boundary of the ROI using a constant interval δb . Finally, a Lebesgue measure can be assigned to the space of line transversals through $\mathcal{A} = [0, L]^2$ to obtain the following track coverage performance measure:

$$\begin{aligned} \mathcal{T}_{\mathcal{A}}^k &= \frac{1}{2} \sum_{\ell=1}^{L/\delta b} \sum_{j=1}^q (-1)^{j+1} \sum_{I_q} \left\{ \psi\left(S_p^{i_1, j}, b_y^\ell\right) + \xi\left(S_p^{i_1, j}, b_{y'}^\ell\right) \right\} \\ &+ \frac{1}{2} \sum_{\ell=0}^{(L/\delta b)-1} \sum_{j=1}^q (-1)^{j+1} \sum_{I_q} \left\{ \zeta\left(S_p^{i_1, j}, b_x^\ell\right) + \rho\left(S_p^{i_1, j}, b_{x'}^\ell\right) \right\} \end{aligned} \quad (8)$$

where $q = n!/(n-k)!k!$ is the binomial coefficient n choose k , and $S_p^{i_1}$ denotes the i_1 th p -subset of S (see [23] for the definition of p -subset). Set I_q contains all $[q!/(q-j)!j!]$ distinct integer j -tuples (i_1, \dots, i_j) satisfying $1 \leq i_1 < i_2 \leq q$. The proof for (8) is based on the principle of inclusion-exclusion and can be found in [8].

The track coverage measure (8) is a trigonometric function of the sensors' positions and detection ranges that can be efficiently optimized via sequential quadratic programming, as shown in [8]. Aside from assuming deterministic sensors' positions, (8) differs from the performance function in (4) in that it uses a sensor-centric approach instead of a track-centric approach. This paper shows that, when applied to a common problem formulation described in the next section, the track-centric approach obtains the same probability of track detection as the sensor-centric approach but is more computationally efficient.

III. PROBLEM FORMULATION AND ASSUMPTIONS

The track detection problem treated in this paper is to determine the probability that a random target moving at constant speed and heading through \mathcal{A} will lead to k independent detections in a network of $n \geq k$ omnidirectional sensors that are randomly distributed in \mathcal{A} . The problem formulation is in 2-D Euclidean space and relies on the following assumptions: 1) The target moves with constant speed $V > 0$ and heading θ ; 2) the ROI is a square, $\mathcal{A} = [0, L]^2$; 3) the sensors' positions, $\mathbf{x}_j \in \mathbb{R}^2$, $j = 1, \dots, n$ are identically and independently distributed (i.i.d.) random vectors; 4) the FOV of each sensor can be represented by a circle, $\mathcal{C}(\mathbf{x}_j, r)$; 5) the probability of detection everywhere in $\mathcal{C}(\mathbf{x}_j, r)$ is equal to one; and 6) the sensors remain in \mathcal{A} until the target has traversed \mathcal{A} .

The sensor network is represented by the family of circles $S = \{\mathcal{C}_1, \dots, \mathcal{C}_n\}$, where $\mathcal{C}_j = \mathcal{C}(\mathbf{x}_j, r)$, with r being a known constant. The probability of the j th sensor being located at a random position $\mathbf{x}_j = [x_j \ y_j]^T$ is described by pdf $f_{\mathbf{x}}(\mathbf{x}_j)$. The complexity of the spatiotemporal track model is a function of the size of the ROI and of the expected target dynamics. Based on assumptions 1) and 6), every possible target track can be represented by a ray or half-line $\mathcal{R}_\theta(\mathbf{x}_{T_0})$ in \mathbb{R}_+^2 , with slope θ , and intercept \mathbf{x}_{T_0} (Fig. 2). Because the track parameters, V , θ , and \mathbf{x}_{T_0} are typically uncorrelated, information about the target track is provided by pdfs $f_V(V)$, $f_\theta(\theta)$, and $f_T(\mathbf{x}_{T_0})$. Without loss of generality, the initial target position can be assumed to be an element of the boundary set of \mathcal{A} in \mathbb{R}^2 , denoted by $\partial\mathcal{A}$. Thus, letting $t = t_0$ when the target first enters \mathcal{A} , it follows that $\mathbf{x}_T(t_0) = \mathbf{x}_{T_0} \in \partial\mathcal{A}$. Then, a detection event by the j th sensor, denoted by $D_j = 1$, occurs with probability one when $\mathcal{R}_\theta(\mathbf{x}_{T_0}) \cap \mathcal{C}(\mathbf{x}_j, r) \neq \emptyset$.

In the next section, the probability of track detection in \mathcal{A} is derived by viewing target tracks as Poisson flats, thereby extending the geometric-transversal approach to the case of random sensors' positions and random track parameters.

IV. PROBABILISTIC TRACK COVERAGE

Poisson flats are random arrangements of hyperplanes placed in \mathbb{R}^d according to a Poisson law. More precisely, a j -dimensional flat in \mathbb{R}^d is a j -dimensional linear manifold in \mathbb{R}^d , and a Poisson j -flat process with $d/2 \leq r < d - 1$ in \mathbb{R}^d is a Poisson point process on the phase space of all j -flats in \mathbb{R}^d [24]. The mean j -content of j -flats per unit d -volume is the intensity of the Poisson process. The properties of Poisson flat processes are reviewed in [25]–[28], and of particular interest are Poisson lines randomly placed in the plane, with $j = 1$ and $d = 2$. Then, the Poisson line process is uniquely determined by the process intensity and the chosen probability measure on $[0, \pi)$ [24]. The results more closely related to the problem treated in this paper pertain to the probability that n (i.i.d.) Poisson flats meeting a fixed ball in \mathbb{R}^d have a common point inside the ball [29].

In this section, we seek the probability that Poisson lines in \mathbb{R}^2 meet at least k circles in the family $S = \{\mathcal{C}_1, \dots, \mathcal{C}_n\}$, which are randomly placed in \mathcal{A} according to $f_{\mathbf{x}}(\mathbf{x}_j)$. The probability of track detection is obtained by formulating the intensity of the Poisson line process in terms of the coverage cones generated by the circles in S . In the next section, this approach is used to derive the probability of having at least

one track detection when the y -intercept b_y is fixed and known. Then, in Section IV-B, the probability of at least k detections occurring for any random track in \mathcal{A} is obtained using the theory of Bernoulli trials and the geometric-transversal approach reviewed in Section II-B.

A. Probability of Track Detection by a Single Sensor for a Fixed Track Intercept

We first derive the probability that a *single* ray $\mathcal{R}_\theta(\mathbf{x}_{T_0})$ with a fixed and known intercept $\mathbf{x}_{T_0} \in \partial\mathcal{A}$, and a random angle $\theta \in [0, \pi/2]$ with pdf $f_\theta(\theta)$, will intersect a circle $\mathcal{C}(\mathbf{x}_j, r)$ that is placed at a random position $\mathbf{x}_j \in \mathcal{A}$ with pdf $f_{\mathbf{x}}(\mathbf{x}_j)$. The approach presented in this paper builds on the novel observation that the experiment of placing ray $\mathcal{R}_\theta(\mathbf{x}_{T_0})$ in \mathbb{R}_+^2 is analogous to the experiment of placing random points on a line, because $\mathcal{R}_\theta(\mathbf{x}_{T_0})$ can be viewed as a point in θ -phase space. Based on this observation, the theory of random Poisson points and repeated trials can be applied to the target tracks, which can be considered as Poisson flats. Subsequently, the approach in Section II-B can be extended to the probabilistic track coverage problem formulated in Section III.

From the theory of Poisson distributions, reviewed comprehensively in [14] and [30], if mI points are placed independently and at random on a line of finite length I , denoted by interval $(0, I)$, then the probability that any one of these points lies in an interval (i_1, i_2) of length l is l/I . By the binomial distribution law, the probability that exactly k of the mI points are found in the interval of length l is

$$\Pr(k \text{ points in } (i_1, i_2)) = \frac{(mI)!}{k!(mI-k)!} \left(\frac{l}{I}\right)^k \left(1 - \frac{l}{I}\right)^{mI-k} \quad (9)$$

and, as $I \rightarrow \infty$, (9) approaches the Poisson distribution with parameter ϕ

$$P(k, \phi) = \frac{\phi^k}{k!} e^{-\phi} \quad (10)$$

where ϕ represents the expected value of k [30, p. 94]. The Poisson distribution also holds for inhomogeneous processes, such as the experiment of placing points that are not uniformly distributed on a line [14, p. 28]. Letting z denote a coordinate along the line and performing a one-to-one transformation, it can be shown that (10) also holds for points distributed on a line with a density $f(z)$ [14, p. 28]. In this case, the expected number of points that fall in an interval (z_1, z_2) is

$$\phi = \int_{z_1}^{z_2} f(z) dz \quad (11)$$

which is the corresponding parameter for the Poisson distribution (10).

It was also shown in [14, p. 86] that the Poisson distribution in (10) can be used to determine the probability that points distributed in a plane, or a volume, fall in a given small region, based solely on coverage factor ϕ . The coverage factor of a spatial Poisson process can be defined as the expected value of the number of points that fall in a small region or subset of a Euclidean space [14, p. 29]. Based on assumptions 4)

and 5) in Section III, every point that falls in this region corresponds to a detection event $D_j = 1$. Therefore, by defining a suitable coverage factor, the Poisson distribution can be used to determine the probability of hitting a static target or that of detecting a moving target in an ROI based on the covered area, as shown in [9] and [14], respectively. Let E denote the experiment of placing a circle \mathcal{C}_j at \mathbf{x}_j . We next determine the probability of the subsequent success of a detection event ($D_j = 1$), such that multiple detections by n sensors can be viewed as independent trials of E , as shown in Section IV-B.

Target tracks through \mathbf{x}_{T_0} are viewed as Poisson flats that are placed in the open cone or half-space $\{(x, y) | x > 0\} \cup \{\mathbf{x}_{T_0}\}$ with a density $f_\theta(\theta)$. In θ -phase space, coverage cone $K(\mathcal{C}_j, \mathbf{x}_{T_0})$ can be viewed as an interval of length $\psi(\mathcal{C}_j, \mathbf{x}_{T_0}) = 2\alpha_j$, randomly placed in $[0, \pi]$. Because ψ is a function of random variable \mathbf{x}_j , the coverage cone is a random interval. Thus, the expected number of Poisson flats that fall in $K(\mathcal{C}_j, \mathbf{x}_{T_0})$ can be obtained by writing its endpoints, or extremals, in rectangular coordinates through a change of variables, and by taking the expectation with respect to \mathbf{x}_j , using pdf $f_{\mathbf{x}}(\mathbf{x}_j)$. Then, from (11), the probability of a detection event $D_j = 1$ can be obtained from a Poisson distribution with coverage factor

$$\begin{aligned} \phi_s(\mathbf{x}_{T_0}) &= \mathbb{E}_{\mathbf{x}_j} \left[\int_{\gamma_j - \alpha_j}^{\gamma_j + \alpha_j} f_\theta(\theta) d\theta \right] \\ &= \int_{\mathcal{A}} f_{\mathbf{x}}(\mathbf{x}_j) \int_{g_1(\mathbf{x}_j, \mathbf{x}_{T_0})}^{g_2(\mathbf{x}_j, \mathbf{x}_{T_0})} f_\theta(\theta) d\theta d\mathbf{x}_j \quad (12) \end{aligned}$$

where the limits of integration in rectangular coordinates

$$\begin{aligned} g_{1,2}(\mathbf{x}_j, \mathbf{x}_{T_0}) &\equiv \gamma_j \pm \alpha_j = \sin^{-1} [(y_j - b_y) / \|\mathbf{x}_j\|] \\ &\quad \pm \sin^{-1} (r / \|\mathbf{x}_j - \mathbf{x}_{T_0}\|) \quad (13) \end{aligned}$$

are the extremals of $K(\mathcal{C}_j, \mathbf{x}_{T_0})$ and are derived from the coverage cone equations in Section II-B. The coverage factor (12) represents the expected number of rays that fall in $K(\mathcal{C}_j, \mathbf{x}_{T_0})$, as well as the approximate probability that at least one ray $\mathcal{R}_\theta(\mathbf{x}_{T_0})$ will both fall in $K(\mathcal{C}_j, \mathbf{x}_{T_0})$ and intersect \mathcal{C}_j . In fact, from (10), the probability of having at least one track detection can be approximated as follows:

$$\begin{aligned} &\Pr \left(\sum_{j=1}^n D_j > 0 \mid \mathbf{x}_{T_0} \in \partial\mathcal{A} \right) \\ &= \sum_{k=1}^{\infty} P(k, \phi_s) = 1 - P(0, \phi_s) = 1 - e^{-\phi_s} \\ &= 1 - \sum_{i=0}^{\infty} \frac{(-\phi_s)^i}{i!} \approx \phi_s, \quad \text{for } \phi_s \ll 1 \quad (14) \end{aligned}$$

using the Maclaurin series. The results in this section are utilized in the next section to obtain the probability of multiple track detections using Bernoulli trials.

B. Probability of Multiple Track Detections by a Probabilistic Sensor Network

In the theory of probability, the concept of repeated trials can be interpreted as the creation of an experiment defined as $E = E_1 \times \cdots \times E_n$, where \times denotes the Cartesian product and E is obtained by combination of n experiments E_1, \dots, E_n [30]. Then, E is a new experiment whose event consists of all of the Cartesian products between all events of all n experiments, E_1, \dots, E_n , as well as their unions and intersections. A special case of repeated trials is that in which the same experiment is repeated n times through n independent trials [30]. In this case, suppose that E denotes a Bernoulli experiment that has only two possible mutually exclusive outcomes, i.e., B is an event of E such that if $\Pr(B) = p$ and $\Pr(\bar{B}) = q$, then $p + q = 1$, where \bar{B} denotes the complement of B in E . Then, if E is repeated n independent times, the product space of the resulting experiment is $E^n = E \times \cdots \times E$, and the probability that event B occurs exactly k times is given by

$$\begin{aligned} \Pr(B \text{ occurs } k \text{ times in any order}) &= \binom{n}{k} p^k q^{n-k} \\ &= \frac{n!}{k!(n-k)!} p^k q^{n-k} \quad (15) \end{aligned}$$

which is a fundamental result in Bernoulli trials (see [30, p. 53] for the proof).

Assuming that all n sensors in S are independently and identically sampled from the same distribution $f_{\mathbf{x}}(\mathbf{x}_j)$, multiple detections can be viewed as repeated trials of the same experiment E (defined in Section IV-A). Then, the probability that a detection event occurs exactly k times, in any order, can be obtained from (14) and (15) and is given by

$$\Pr \left(\sum_{j=1}^n D_j = k \mid \mathbf{x}_{T_0} \in \partial\mathcal{A} \right) = \binom{n}{k} \phi_s^k (1 - \phi_s)^{n-k} \quad (16)$$

where ϕ_s is defined in (12). Because the probability of having at least k detections is the complementary probability of having $0, 1, \dots, k-1$ detections, it follows that

$$\begin{aligned} &\Pr \left(\sum_{j=1}^n D_j \geq k \mid \mathbf{x}_{T_0} \in \partial\mathcal{A} \right) \\ &= 1 - \sum_{m=0}^{k-1} \Pr \left(\sum_{j=1}^n D_j = m \mid \mathbf{x}_{T_0} \in \partial\mathcal{A} \right) \\ &= 1 - \sum_{m=0}^{k-1} \frac{n!}{m!(n-m)!} \phi_s^m (1 - \phi_s)^{n-m}. \quad (17) \end{aligned}$$

If n and k are large, the aforementioned equation may be hard to compute numerically because of the repeated factorials inside the summation. In this case, Poisson's theorem can be used to derive a convenient approximation to (17) for networks with $\phi_s \ll 1$ and $n \gg 1$. As reviewed in more detail in [30, p. 113], Poisson's theorem states that if $p \rightarrow 0$ and $n \rightarrow \infty$, such that

$np \rightarrow \lambda$, where λ is a constant, then the probability in (15) can be approximated by the limit

$$\frac{n!}{k!(n-k)!} p^k q^{n-k} \rightarrow e^{-\lambda} \frac{\lambda^k}{k!}, \quad \text{as } n \rightarrow \infty, \quad (18)$$

and $k = 0, 1, 2, \dots$

Thus, by substituting (12) in (15) and by rewriting (18) in terms of m , the probability of having at least k detections in (17) can be approximated by

$$\Pr \left(\sum_{j=1}^n D_j \geq k \mid \mathbf{x}_{T_0} \in \partial \mathcal{A} \right) \approx 1 - e^{-n\phi_s} \sum_{m=0}^{k-1} \frac{(n\phi_s)^m}{m!} \quad (19)$$

assuming that ϕ_s and n diverge to the two extremes, i.e., $\phi_s \rightarrow 0$ and $n \rightarrow \infty$, such that $n\phi_s$ remains constant.

So far, all probabilities are conditioned on the target entering \mathcal{A} at a fixed and known position $\mathbf{x}_{T_0} \in \partial \mathcal{A}$. Consider now the case in which \mathbf{x}_{T_0} is also a random variable, and the probability that the target enters \mathcal{A} at \mathbf{x}_{T_0} is described by a pdf $f_T(\mathbf{x}_{T_0})$ defined over boundary set $\partial \mathcal{A}$. Then, the probability that a target in \mathcal{A} is detected at least k times is obtained by marginalizing (19) over all possible values of \mathbf{x}_{T_0} , i.e.,

$$P_s = \Pr \left(\sum_{j=1}^n D_j \geq k \mid \mathbf{x}_T(t) \in \mathcal{A} \right) = 1 - \int_{\partial \mathcal{A}} f_T(\mathbf{x}_{T_0}) e^{-n\phi_s(\mathbf{x}_{T_0})} \sum_{m=0}^{k-1} \frac{[n\phi_s(\mathbf{x}_{T_0})]^m}{m!} d\mathbf{x}_{T_0} \quad (20)$$

The aforementioned performance function represents the track coverage of a probabilistic sensor network with pdf $f_{\mathbf{x}}(\mathbf{x}_j)$, computed in terms of coverage cones with extremals g_1 and g_2 , as shown in (12) and (13). Its deterministic counterpart in (8) represents the track coverage of a sensor network as a function of deterministic sensor positions in \mathcal{A} . While (8) assumes that track parameters \mathbf{x}_{T_0} and θ are uniformly distributed over their ranges [8], the newly derived performance function in (20) is applicable to random tracks with nonuniform pdfs $f_T(\mathbf{x}_{T_0})$ and $f_\theta(\theta)$. The performance function in (20) can also be applied to multiple targets, provided that all targets have track parameters characterized by the same pdfs, and that all detections are assigned to the corresponding targets by means of a multisensor–multitarget data association algorithm [31]–[33]. Furthermore, the approach presented in this section can be extended to maneuvering targets using a Markov target model, as will be shown in a separate paper.

The next section shows that the approach presented in this section obtains the same probability of track detection obtained by the distributed-search approach reviewed in Section II-A.

V. RELATIONSHIP BETWEEN GEOMETRIC-TRANSVERSAL AND DISTRIBUTED-SEARCH APPROACHES

The geometric-transversal approach in Section IV can be considered as sensor centric because it is based on a cone

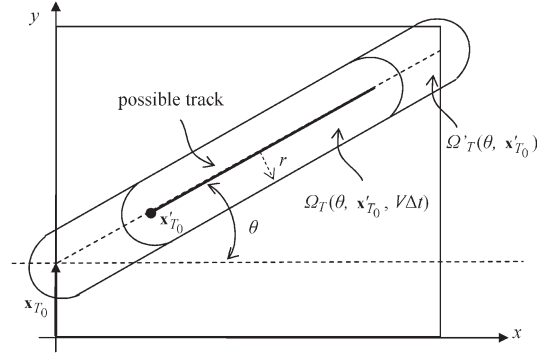


Fig. 3. Transformation from \mathbf{x}'_{T_0} to \mathbf{x}_{T_0} and from Ω_T to Ω'_T .

representation of the tracks detected by each sensor in the network. The distributed-search approach presented in [9], on the other hand, is based on an area representation of the sensors' positions that detect each target track in \mathcal{A} . Therefore, it can be considered as a track-centric approach. In this section, we show that the two approaches are equivalent under the same problem formulation and assumptions described in Section III. In particular, we prove that the probability of track detection in (20) is equivalent to the probability of track detection derived from (4) using the distributed-search approach in [9].

As a first step, the performance function in (4) is applied to the problem formulation in Section III, in which sensors can detect the target at any time $t_0 \leq t \leq t_f$ in \mathcal{A} . Then, (4) can be used to represent the probability of track detection by letting $(t_f - t_0) > \sqrt{L^2/2V_{\min}}$, and by imposing the condition that the initial target position is on the ROI boundary. The new probability of track detection is obtained by performing a change of variables from the initial position $\mathbf{x}'_{T_0} \in \mathcal{A}$, as defined in Section II-A, to the initial position $\mathbf{x}_{T_0} \in \partial \mathcal{A}$, as defined in Section IV. When \mathbf{x}_{T_0} is on the y -axis, as shown by the example in Fig. 3, this change of variables amounts to the transformation $\mathbf{x}_{T_0} = [0 \ (x'_0 - y'_0 \tan \theta)]^T$, where $\mathbf{x}'_{T_0} = [x'_0 \ y'_0]^T$ and θ are sampled from pdfs $f_T(\mathbf{x}'_{T_0})$ and $f_\theta(\theta)$, respectively. Similar transformations can be obtained for all $\mathbf{x}_{T_0} \in \partial \mathcal{A}$. In every case, \mathbf{x}_{T_0} is independent of V . Thus, the joint pdf of \mathbf{x}_{T_0} and θ , denoted by $g_T(\mathbf{x}_{T_0}, \theta)$, is a derived distribution that can be computed from $f_\theta(\theta)$ and $f_T(\mathbf{x}'_{T_0})$, using the aforementioned transformations to express \mathbf{x}_{T_0} in terms of \mathbf{x}'_{T_0} . The standard procedure for deriving a distribution using the Jacobian of the transformation is described in [18, Section 1.7].

Based on assumption 6), the detection region $\Omega_T(\mathbf{x}'_{T_0}, \theta, V\Delta t)$, defined in Section II-A, is transformed into a new detection region that is independent of V and Δt , and is denoted by $\Omega'_T(\mathbf{x}_{T_0}, \theta)$, as shown in Fig. 3. Where, $\Omega'_T(\mathbf{x}_{T_0}, \theta)$ is obtained by growing the entire track isotropically by r from the target's point of entry to its exit point in \mathcal{A} . As a result, the coverage factor in (3) is integrated over the new detection region and can be written as

$$\phi'_t(\mathbf{x}_{T_0}, \theta) = \int_{\Omega'_T(\mathbf{x}_{T_0}, \theta)} f_{\mathbf{x}}(\mathbf{x}_j) d\mathbf{x}_j. \quad (21)$$

When the coverage factor (21) and the derived distribution $g_T(\mathbf{x}_{T_0}, \theta)$ are substituted in (4), the probability of track

detection obtained by the distributed-search approach can be simplified to

$$\begin{aligned}
 P_t &= 1 - \int_0^{2\pi} \int_{\partial\mathcal{A}} e^{-n\phi'_t(\mathbf{x}_{T_0}, \theta)} g_T(\mathbf{x}_{T_0}, \theta) \\
 &\quad \times \sum_{m=0}^{k-1} \frac{[n\phi'_t(\mathbf{x}_{T_0}, \theta)]^m}{m!} d\mathbf{x}_{T_0} d\theta \int_{V_{\min}}^{V_{\max}} f_V(V) dV \\
 &= 1 - \int_0^{2\pi} \int_{\partial\mathcal{A}} e^{-n\phi'_t(\mathbf{x}_{T_0}, \theta)} g_T(\mathbf{x}_{T_0}, \theta) \\
 &\quad \times \sum_{m=0}^{k-1} \frac{[n\phi'_t(\mathbf{x}_{T_0}, \theta)]^m}{m!} d\mathbf{x}_{T_0} d\theta \quad (22)
 \end{aligned}$$

because the integral of the pdf $f_V(V)$ over its limits is always equal to one.

Now, let $\phi''_t(\mathbf{x}_{T_0})$ denote the expected coverage factor as a function of intercept \mathbf{x}_{T_0} , which is obtained by applying the expected value rule [34, p. 145] to the function (21), i.e.,

$$\begin{aligned}
 \phi''_t(\mathbf{x}_{T_0}) &= \int_0^{2\pi} \phi'_t(\mathbf{x}_{T_0}, \theta) f_\theta(\theta) d\theta \\
 &= \int_0^{2\pi} f_\theta(\theta) \int_{\Omega'_T(\mathbf{x}_{T_0}, \theta)} f_{\mathbf{x}}(\mathbf{x}_j) d\mathbf{x}_j d\theta \quad (23)
 \end{aligned}$$

where $\theta \in [0, 2\pi]$ when $\mathcal{R}_\theta(\mathbf{x}_{T_0}) \in \mathbb{R}^2_+$. Then, (22) can be rewritten as

$$\begin{aligned}
 P_t &= 1 - \int_{\partial\mathcal{A}} e^{-n\phi''_t(\mathbf{x}_{T_0}, \theta)} \\
 &\quad \times \sum_{m=0}^{k-1} \frac{[n\phi''_t(\mathbf{x}_{T_0}, \theta)]^m}{m!} \int_0^{2\pi} g_T(\mathbf{x}_{T_0}, \theta) d\theta d\mathbf{x}_{T_0} \\
 &= 1 - \int_{\partial\mathcal{A}} f_T(\mathbf{x}_{T_0}) e^{-n\phi''_t(\mathbf{x}_{T_0}, \theta)} \sum_{m=0}^{k-1} \frac{[n\phi''_t(\mathbf{x}_{T_0}, \theta)]^m}{m!} d\mathbf{x}_{T_0} \quad (24)
 \end{aligned}$$

because the inner integral in (24) amounts to marginalizing the joint pdf $g_T(\mathbf{x}_{T_0}, \theta)$ over θ , which results in the marginal distribution $f_T(\mathbf{x}_{T_0})$.

Comparing (24) to (20), it can be seen that the distributed-search and geometric-transversal approaches lead to the same equation for the probability of track detection, provided $\phi_s(\mathbf{x}_{T_0}) = \phi''_t(\mathbf{x}_{T_0})$. Without loss of generality, we prove that this equality holds for the case of $\mathbf{x}_{T_0} = \mathbf{0}$. The same proof can be applied to any $\mathbf{x}_{T_0} \in \partial\mathcal{A}$ by translating the xy -coordinate frame such that its origin coincides with \mathbf{x}_{T_0} . When $\mathbf{x}_{T_0} = \mathbf{0}$, the coverage factors ϕ_s and ϕ''_t are two constants that can be evaluated from the triple integrals (12) and (23), respectively. Because the sensors' positions are independently and identi-

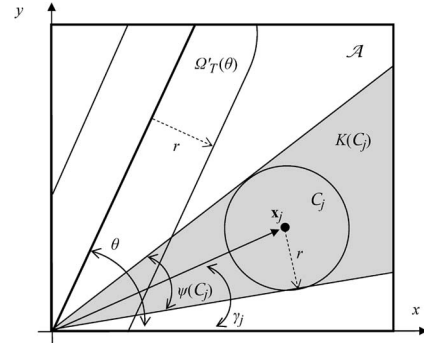


Fig. 4. Detection region $\Omega'_T(\theta)$ and coverage cone $K(C_j)$ for $\mathbf{x}_{T_0} = \mathbf{0}$.

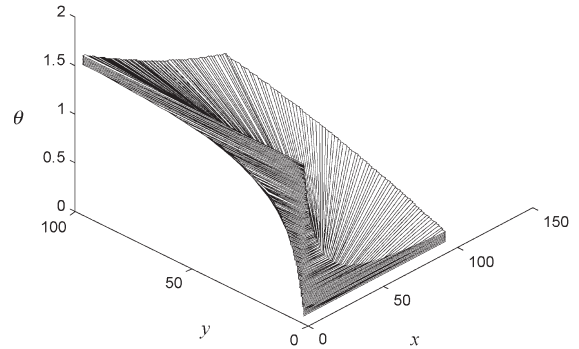


Fig. 5. Region of integration of $\phi''_t(\mathbf{x}_{T_0})$.

cally sampled from $f_{\mathbf{x}}(\mathbf{x}_j)$, the coverage factor in (12), obtained by the geometric-transversal approach, can be written as

$$\phi_s = \int_{\mathcal{A}} \int_{g_1(\mathbf{x}_j)}^{g_2(\mathbf{x}_j)} f_{\mathbf{x}}(\mathbf{x}_j) f_\theta(\theta) d\theta d\mathbf{x}_j, \quad \text{for } \mathbf{x}_{T_0} = \mathbf{0}. \quad (25)$$

Because \mathbf{x}_j and θ are independent random variables, the coverage factor in (23), obtained by the distributed-search approach, can be written as

$$\phi''_t = \int_0^{2\pi} \int_{\Omega'_T(\theta)} f_\theta(\theta) f_{\mathbf{x}}(\mathbf{x}_j) d\mathbf{x}_j d\theta, \quad \text{for } \mathbf{x}_{T_0} = \mathbf{0}. \quad (26)$$

Furthermore, the integrands of (25) and (26) each represent the joint pdf of \mathbf{x}_j and θ because $f_{\mathbf{x},\theta}(\mathbf{x}_j, \theta) = f_{\mathbf{x}}(\mathbf{x}_j) f_\theta(\theta)$. It follows that coverage factors ϕ_s and ϕ''_t each represent the probability mass of \mathbf{x}_j and θ in the 3-D regions of integration of (25) and (26), respectively. Specifically, the probability mass of two random variables \mathbf{x}_j and θ in a 3-D region $\mathcal{V} \subset \mathbb{R}^3$ is defined as the probability that point (\mathbf{x}_j, θ) is in \mathcal{V} , given the density $f_{\mathbf{x},\theta}(\mathbf{x}_j, \theta)$ [30, p. 172]. From (13) and (25), the region of integration of ϕ_s is the region spanned by the coverage cone $K(C_j, \mathbf{x}_{T_0} = \mathbf{0}) \equiv K(C_j)$ for all $\mathbf{x}_j \in \mathcal{A}$. Thus, the projection of this region of integration onto \mathcal{A} at a sample value of \mathbf{x}_j is the coverage cone $K(C_j)$ shown in Fig. 4. From (21) and (26), the region of integration of ϕ''_t is the region spanned by $\Omega'_T(\theta)$ for all $\theta \in [0, \pi/2]$. Thus, the projection of this region of integration onto \mathcal{A} at a sample value of θ is the detection region $\Omega'_T(\theta)$ shown in Fig. 4. As an example, the region of integration of ϕ''_t is shown in Fig. 5 for $L = 105$ and $r = 5$.

From the probability masses in (25) and (26), it can be seen that ϕ_s and ϕ_t'' are equivalent, provided that the region of integration in (25) is equivalent to that in (26). This last step of the proof is carried out by showing that the volume of the region of integration in (25), defined as

$$v_s = \int_{\mathcal{A}} \int_{g_1(\mathbf{x}_j)}^{g_2(\mathbf{x}_j)} d\theta d\mathbf{x}_j \quad (27)$$

is equivalent to the volume of the region of integration in (26), defined as

$$v_t = \int_0^{2\pi} \int_{\Omega_T'(\theta)} d\mathbf{x}_j d\theta \quad (28)$$

In order to avoid singularities, the aforementioned volumes are evaluated by assuming that $\mathcal{C}_j \in \mathcal{A}$, i.e., letting $r \leq x_j$ and $y_j \leq L - r$. Using the notation in Fig. 4, the limits in (27) can be expressed in polar coordinates, and (27) can be simplified as follows:

$$v_s = \int_{\mathcal{A}} \int_{\gamma_j - \psi_j/2}^{\gamma_j + \psi_j/2} d\theta d\mathbf{x}_j = \int_{\mathcal{A}} 2 \arcsin\left(\frac{r}{\|\mathbf{x}_j\|}\right) d\mathbf{x}_j. \quad (29)$$

Because the geometry of $\Omega_T'(\theta)$ changes with θ , (28) is evaluated by dividing the range of θ into five intervals, such that

$$\theta \in [0, \pi/2] = [\theta_0, \theta_1] \cup [\theta_1, \theta_2] \cup [\theta_2, \theta_3] \cup [\theta_3, \theta_4] \cup [\theta_4, \theta_5] \quad (30)$$

where $\theta_0 = 0$, $\theta_5 = \pi/2$, and

$$\begin{aligned} \theta_1 &\equiv \arcsin \frac{r}{\sqrt{(L-r)^2 + r^2}} + \arctan \frac{r}{(L-r)} \\ \theta_2 &\equiv \frac{\pi}{4} - \arcsin \frac{r}{\sqrt{2}(L-r)} \\ \theta_3 &\equiv \arcsin \frac{r}{\sqrt{(L-r)^2 + r^2}} + \frac{\pi}{4} \\ \theta_4 &\equiv \arctan \frac{(L-r)}{r} - \arcsin \frac{r}{\sqrt{r^2 + (L-r)^2}}. \end{aligned}$$

Then, the volume in (28) can be written as

$$v_t = \sum_{i=0}^4 \int_{\theta_i}^{\theta_{i+1}} \int_{\Omega_T'(\theta)} d\mathbf{x}_j d\theta = \sum_{i=0}^4 \int_{\theta_i}^{\theta_{i+1}} f_{i+1}(\theta) d\theta \quad (31)$$

where

$$\begin{aligned} f_1(\theta) &\equiv \frac{1}{2} \left(L \tan \theta + \frac{2r}{\cos \theta} - 2r \right) (L-2r) \\ f_2(\theta) &\equiv (L-2r)^2 - \frac{1}{2} \left\{ \left(L-r - \frac{r \cos \theta + r}{\sin \theta} \right) \right. \\ &\quad \times \left[(L-r) \tan \theta - \frac{r}{\cos \theta} - r \right] + (L-2r) \\ &\quad \left. \times \left[2(L-r) - L \tan \theta - \frac{2r}{\cos \theta} \right] \right\} \quad (32) \end{aligned}$$

$$\begin{aligned} f_3(\theta) &\equiv (L-2r)^2 - \frac{1}{2} \left\{ \left[(L-r) - \frac{r \cos \theta + r}{\sin \theta} \right] \right. \\ &\quad \times \left[(L-r) \tan \theta - \frac{r}{\cos \theta} - r \right] \\ &\quad \left. + \left[\frac{(L-r) \cos \theta - r}{\sin \theta} - r \right] \left(L-r-r \tan \theta - \frac{r}{\cos \theta} \right) \right\} \\ f_4(\theta) &\equiv (L-2r)^2 - \frac{1}{2} \left\{ (L-2r) \left(\frac{L \cos \theta + 2r}{\sin \theta} - 2r \right) \right. \\ &\quad \left. + \left[\frac{(L-r) \cos \theta - r}{\sin \theta} - r \right] \left(L-r-r \tan \theta - \frac{r}{\cos \theta} \right) \right\} \\ f_5(\theta) &\equiv \frac{1}{2} (L-2r) \left(\frac{L \cos \theta + 2r}{\sin \theta} - 2r \right). \quad (33) \end{aligned}$$

Finally, v_t in (31) is integrated analytically (the analytic solution is omitted for brevity), and its value is shown in Fig. 6(a) for representative values of parameters L and r . The volume v_s in (29) is first integrated analytically with respect to y_j . Then, because an explicit solution for the outer integral in x_j could not be determined, v_s is computed using the recursive adaptive Lobatto quadrature, which approximates the outer integral to within an error of $O(10^{-6})$ [35]. For comparison, the value of v_s is shown in Fig. 6(b) using the same parameter values used for v_t in Fig. 6(a). For all parameter values considered in the simulations, the difference between v_s and v_t is on the order of the Lobatto quadrature error. Thus, it can be concluded that the two volumes are equivalent and that $\phi_s = \phi_t''$. It follows that the probabilities of track detection in (20) and (24), obtained by the geometric-transversal and distributed-search approaches, respectively, are equivalent. The two approaches differ in the manner by which they integrate the joint sensor-target pdf over the space of all possible target tracks and sensors' positions. As illustrated by the corresponding regions of integration, the distributed-search approach considers the area containing all sensors' positions that detect a single track, and then integrates the joint pdf over all possible target tracks. The geometric-transversal approach considers the cone containing all target tracks that are detected by a single sensor position, and then integrates the joint pdf over all possible sensors' positions in \mathcal{A} .

In the next section, the theoretical results are validated through numerical simulations. These simulations confirm that the two approaches lead to the same probability of track detection and can thus be reliably utilized to optimize the design and deployment of cooperative sensor networks.

VI. NUMERICAL SIMULATIONS AND RESULTS

The theoretical results obtained in the previous sections are demonstrated through numerical simulations involving probabilistic and sampled networks, for different sensor parameters and pdfs. In Section VI-A, the new performance function derived by the geometric-transversal approach in Section IV is evaluated numerically and is compared to the performance function obtained by the distributed-search approach in Section V. The numerical results show that the two performance functions and corresponding coverage factors are always equivalent but require different computation times. As shown in [8], the track coverage function in (8) can be used to efficiently deploy small- to medium-size networks. When the sensor network is very large or subject to significant errors

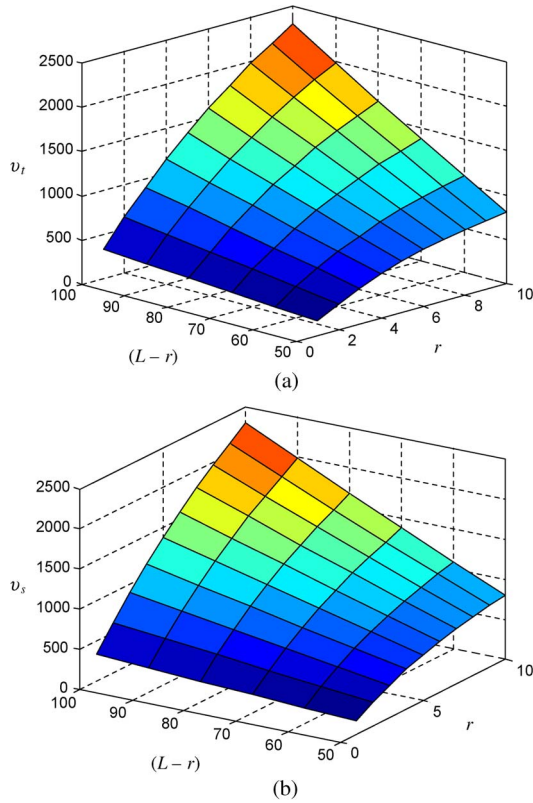


Fig. 6. (a) Volume v_t is compared to (b) v_s for a range of parameters L and r .

and uncertainties, the pdf $f_{\mathbf{x}}(\mathbf{x}_j)$ can be used to deploy sensor networks via sampling [36]. In this case, an optimal pdf can be obtained by optimizing the probabilistic track coverage function in (20) with respect to a parameterized Gaussian mixture. This approach is demonstrated in Section VI-B by considering several examples of sensor deployments obtained by sampling $f_{\mathbf{x}}(\mathbf{x}_j)$ using finite mixture sampling [37, Section 1.4] and entropic sampling [36] techniques. For each deployment, the probability of track detection is evaluated numerically using the geometric-transversal and distributed-search approaches.

A. Probability of Track Detection by Probabilistic Sensor Networks

In this section, the proof in Section V is validated by demonstrating that the probability of track detection P_s in (20) and the probability of track detection P_t in (24) are equivalent for a given pdf $f_{\mathbf{x}}(\mathbf{x}_j)$. It is assumed that the track parameters are unknown and can thus be described by uniform pdfs, $f_T(\mathbf{x}_{T_0})$ and $f_{\theta}(\theta)$ [38]. The ROI is given by $\mathcal{A} = [0, 100]^2$, and all sensors have a constant detection range $r = 5$. The pdf $f_{\mathbf{x}}(\mathbf{x}_j)$ is set equal to zero outside the region $[r, (L-r)]^2 = [5, 95]^2$ to ensure that all FOVs are contained in \mathcal{A} . The number of sensors, n , is varied from 0 to 150, and the number of required detections, k , is varied from zero to ten. The maximum number of sensors (i.e., 150) is chosen such that a network could be contained in \mathcal{A} with little or no overlapping between FOVs. The support of random vector \mathbf{x}_j , given by $[5, 95]^2$, and the support of \mathbf{x}_{T_0} , given by $\partial\mathcal{A}$, are discretized by constant intervals $\Delta\mathbf{x}_j = \Delta\mathbf{x}_{T_0} = [1 \ 1]^T$. The pdf $f_{\mathbf{x}}(\mathbf{x}_j)$ is first modeled

as a uniform distribution over $[5, 95]^2$ and then as a mixed normal pdf

$$f_{\mathbf{x}}(\mathbf{x}_j) = \frac{1}{600\pi} e^{-\frac{(x_j-20)^2}{200} - \frac{(y_j-20)^2}{200}} + \frac{1}{600\pi} e^{-\frac{(x_j-60)^2}{200} - \frac{(y_j-40)^2}{200}} + \frac{1}{600\pi} e^{-\frac{(x_j-75)^2}{200} - \frac{(y_j-75)^2}{200}}. \quad (34)$$

For every pdf model, the probability of track detection P_s in (20) is computed numerically by evaluating the coverage factor in (12) for every discrete value of \mathbf{x}_{T_0} , denoted by $\mathbf{x}_{T_0}^{\ell}$, summing over all discrete values of \mathbf{x}_j , denoted by \mathbf{x}_j^{ℓ} , such that

$$\phi_s(\mathbf{x}_{T_0}^{\ell}) \approx \sum_{\mathbf{x}_j^{\ell} \in \mathcal{A}} \psi(\mathbf{x}_j^{\ell}, \mathbf{x}_{T_0}^{\ell}) f_{\mathbf{x}}(\mathbf{x}_j^{\ell}) \Delta\mathbf{x}_j \quad (35)$$

where opening angle $\psi(\cdot)$ is computed using (7). From (20), the probability of track detection is approximated by

$$P_s \approx 1 - \sum_{\mathbf{x}_{T_0}^{\ell} \in \partial\mathcal{A}} f_T(\mathbf{x}_{T_0}^{\ell}) e^{-n\phi_s(\mathbf{x}_{T_0}^{\ell})} \sum_{m=0}^{k-1} \frac{[n\phi_s(\mathbf{x}_{T_0}^{\ell})]^m}{m!} \Delta\mathbf{x}_{T_0}. \quad (36)$$

For comparison, the probability of track detection in (24) is also computed numerically by discretizing the range of θ , given by $[0, \pi/2]$, using the constant interval $\Delta\theta = 0.01$ rad. The coverage factor in (23) is evaluated by summing over all discrete values of θ , denoted by θ^j , such that

$$\phi_t''(\mathbf{x}_{T_0}^{\ell}) \approx \sum_{\theta^j \in [0, \pi/2]} \Omega_T'(\mathbf{x}_{T_0}^{\ell}, \theta^j) f_{\theta}(\theta^j) \Delta\theta \quad (37)$$

where $\Omega_T'(\cdot)$ is evaluated using f_1 through f_5 in (31). Then, from (24), the probability of track detection is approximated by

$$P_t \approx 1 - \sum_{\mathbf{x}_{T_0}^{\ell} \in \partial\mathcal{A}} f_T(\mathbf{x}_{T_0}^{\ell}) e^{-n\phi_t''(\mathbf{x}_{T_0}^{\ell})} \sum_{m=0}^{k-1} \frac{[n\phi_t''(\mathbf{x}_{T_0}^{\ell})]^m}{m!} \Delta\mathbf{x}_{T_0}. \quad (38)$$

The probabilities of track detection obtained from (36) and (38) are shown in Fig. 7 as a function of n , for a uniform pdf model and $k = 2$. It can be seen that the difference between P_t and P_s is negligibly small. The coverage factors in (35) and (37) are evaluated numerically and compared in Fig. 8. Although the accuracy could be further improved by decreasing the discretization intervals in (36) and (38), it can be concluded that the two approaches provide equivalent probability functions and coverage factors for a uniform pdf. The same conclusion can be drawn for the mixed normal pdf in (34), which leads to the probabilities of track detection shown in Fig. 9. Although the two performance functions P_t and P_s lead to the same value of probability of track detection, P_s typically requires smaller computation times. For example, for a network with $(n, k) = (80, 2)$ and a uniform pdf, P_s in (36) was computed in approximately 0.4 s, while P_t in (38) required approximately 30 s on a Pentium-4 CPU 3.06-GHz computer with 1-GB RAM. For the mixed normal pdf in (34) and $(n, k) = (80, 2)$, P_s and P_t required approximately 0.8 s and 32 s, respectively, on the same computer.

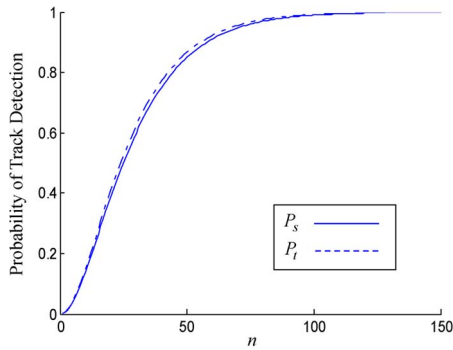


Fig. 7. Comparison between the probability of track detection obtained by the geometric-transversal approach, P_s in (36), and that obtained by the distributed-search approach, P_t in (38), for a uniform pdf and $k = 2$.

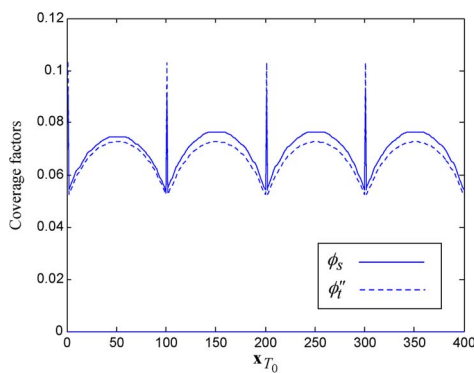


Fig. 8. Comparison between the coverage factor obtained by the geometric-transversal approach, ϕ_s in (35), and that obtained by the distributed-search approach, ϕ'_t in (37), for a uniform pdf and $k = 2$.

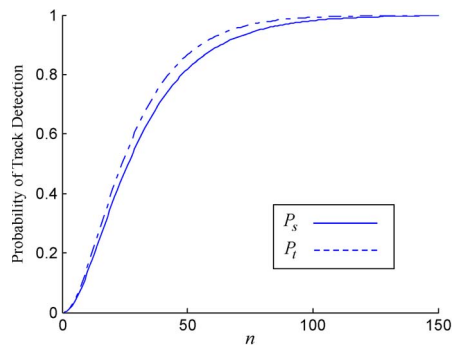


Fig. 9. Comparison between the probability of track detection obtained by the geometric-transversal approach, P_s in (36), and that obtained by the distributed-search approach, P_t in (38), for a mixed normal pdf and $k = 2$.

B. Probability of Track Detection by Sampled Sensor Networks

An effective approach to deploying a large sensor network in an uncertain environment is to sample the pdf $f_{\mathbf{x}}(\mathbf{x}_j)$ to obtain n sensor positions in \mathcal{A} . In this case, the probability of track detection can be optimized with respect to the parameters of a finite mixture model of $f_{\mathbf{x}}(\mathbf{x}_j)$, which is then sampled and used to deploy the sensor network. Because the sampling process greatly influences the configuration of the network, we compare two methods, namely, finite mixture sampling [37, Section 1.4] and entropic sampling [36]. Let vectors $\mathbf{X}_1, \dots, \mathbf{X}_n \in \mathbb{R}^2$

denote the n sensor positions in \mathcal{A} that are sampled randomly from the finite mixture model

$$f_{\mathbf{x}}(\mathbf{x}_j) = \sum_{i=1}^m w_i f_i(\mathbf{x}_j), \quad 0 \leq w_i \leq 1 \quad \forall i, \quad \sum_{i=1}^m w_i = 1. \quad (39)$$

The weights w_1, \dots, w_m are called the mixing proportions, and $f_1(\mathbf{x}_j), \dots, f_m(\mathbf{x}_j)$ are the component densities of the mixture.

In this section, normal mixture models with up to three components are simulated and sampled as follows. In the first technique, referred to as finite mixture sampling [37, Section 1.4], every position \mathbf{X}_j is obtained from the hierarchical model defined as

$$g(\mathbf{x}_j|w) \equiv \begin{cases} f_1(\mathbf{x}_j), & \text{if } w \leq w_1 \\ f_2(\mathbf{x}_j), & \text{if } w_1 < w \leq w_2 \\ \dots & \\ f_n(\mathbf{x}_j), & \text{if } w > w_{n-1} \end{cases} \quad (40)$$

for a random parameter w with a uniform pdf over its range $[0, 1]$. Then, the marginal pdf $g(\mathbf{x}_j)$ has the same distribution as $f_{\mathbf{x}}(\mathbf{x}_j)$, because

$$\begin{aligned} g(\mathbf{x}_j) &= \int_0^1 g(\mathbf{x}_j|w) f_w(w) dw \\ &= \int_0^{w_1} f_1(\mathbf{x}_j) f_w(w) dw + \int_{w_1}^{w_1+w_2} f_2(\mathbf{x}_j) f_w(w) dw \\ &\quad + \dots + \int_{w_1+w_2+\dots+w_{n-1}}^1 f_n(\mathbf{x}_j) f_w(w) dw \\ &= w_1 f_1(\mathbf{x}_j) + w_2 f_2(\mathbf{x}_j) + \dots + w_n f_n(\mathbf{x}_j) = f_{\mathbf{x}}(\mathbf{x}_j) \end{aligned} \quad (41)$$

where $f_w(w) = 1$ if $0 < w < 1$, and $f_w(w) = 0$ otherwise. If the sensor positions are sampled directly from (39), the majority of the sensors cluster near the centers (means) of the pdf components. In order to avoid intersecting FOVs and to obtain independent detections, the new sensors are sampled after biasing the probability using the hierarchical model in (40). Assume that $\mathbf{X}_1, \dots, \mathbf{X}_{j-1}$ have already been sampled, and let W denote a sample of w obtained from $f_w(w)$ using a uniform pseudorandom number generator [39]. Then, for $w_{k-1} < w \leq w_k$, a new sample \mathbf{X}_j is sampled from component $f_k(\mathbf{x}_j)$, which is typically a normal pdf. In order to avoid intersections, the new position \mathbf{X}_j is discarded whenever it results in $\mathcal{C}_j(\mathbf{X}_j, r) \cap [\mathcal{C}_1(\mathbf{X}_1, r) \cup \dots \cup \mathcal{C}_{j-1}(\mathbf{X}_{j-1}, r)] \neq \emptyset$.

Unless n is significantly large, the aforesaid procedure may not produce a sensor distribution that closely represents all of the features of the pdf $f_{\mathbf{x}}(\mathbf{x}_j)$ [36]. A heuristic sampling method was developed in [36] to place sensors sequentially based on the entropy of the posterior pdf in a manner that avoids intersections between the FOVs while capturing the main

features of $f_{\mathbf{x}}(\mathbf{x}_j)$. In this method, every sensor j is placed at the position of maximum conditional entropy, defined as

$$\mathbf{X}_j = \arg \max_{\mathbf{x}} H^{\pi_j}(\mathbf{x}) \equiv - \sum_{\mathbf{x} \in \mathcal{A}} \pi_j(\mathbf{x}|\mathbf{X}_{j-1}) \log \pi_j(\mathbf{x}|\mathbf{X}_{j-1}) \quad (42)$$

for $j = 1, \dots, n$. Where,

$$\pi_j(\mathbf{x}|\mathbf{X}_{j-1}) \propto b_{j-1}(\mathbf{x})\pi_{j-1}(\mathbf{x}|\mathbf{X}_{j-2}) \quad (43)$$

is the posterior pdf updated after placing the $(j - 1)$ th sensor, and $b_j(\mathbf{x})$ is a binary operator that is equal to zero for all $\mathbf{x} \in \mathcal{C}_j$, and is equal to one elsewhere. As in Bayes recursion, at every iteration, the posterior of a previous sensor placement becomes the prior, and the new posterior is used to place an additional sensor, thereby decreasing the probability that multiple sensors are placed at the same location.

Because the sensors' positions are not identically and independently sampled in entropic sampling, the exact probability of track detection cannot be determined by the performance metrics in (20) and (24). After the network is sampled, however, its probability of track detection can be accurately determined from the deterministic track coverage function T_A^k in (8), as reviewed in Section II-B. Using geometric transversals, it was shown in [8] that the probability of track detection of a network deployed at $\mathbf{X}_1, \dots, \mathbf{X}_n$ is given by

$$P_A = \frac{\delta b}{\pi(L + \delta b)} T_A^k. \quad (44)$$

Thus, P_A can be considered as the deterministic counterpart of P_s in (20). Because there currently exists no deterministic counterpart for P_t in (24), P_A is compared to the probability obtained by direct evaluation of detection events D_j 's, denoted by P_k . A logical array or truth table, denoted by B_j , is evaluated such that every element corresponds to a pair of discretized track parameters $(\mathbf{x}_{T_0}^\ell, \theta^j)$ (obtained as explained in Section VI-A), and is set equal to one or zero, depending on whether the track has been detected (one) or missed (zero) by the j th sensor. After the array B_j is obtained for every sampled sensor, the logical array

$$T_k = \left\{ \sum_{j=1}^n B_j \geq k \right\} \quad (45)$$

indicates whether each possible track in \mathcal{A} has been detected by at least k sensors. Then, the number of ones in T_k divided by its number of elements provides the estimate P_k for the probability of track detection.

In the first example, $n = 40$ sensors' positions are sampled from a uniform pdf, $f_{\mathbf{x}}(\mathbf{x}_j)$ using finite mixture and entropic sampling, as shown in Fig. 10(a) and (b), respectively. The probabilities of track detections, P_A and P_k , are shown in Fig. 11 for $r = 5$ and $\mathcal{A} = [0, 100]^2$. From these results, it can be seen that the two approaches lead to the same probability of track detection for both sampling techniques across various values of k . Fig. 11 also shows that, in this case, the network obtained via finite mixture sampling displays better performance than the one sampled via entropic sampling. In the second example, the sensor networks in Fig. 12 are sampled from the normal mixture density in (34). The corresponding probabilities

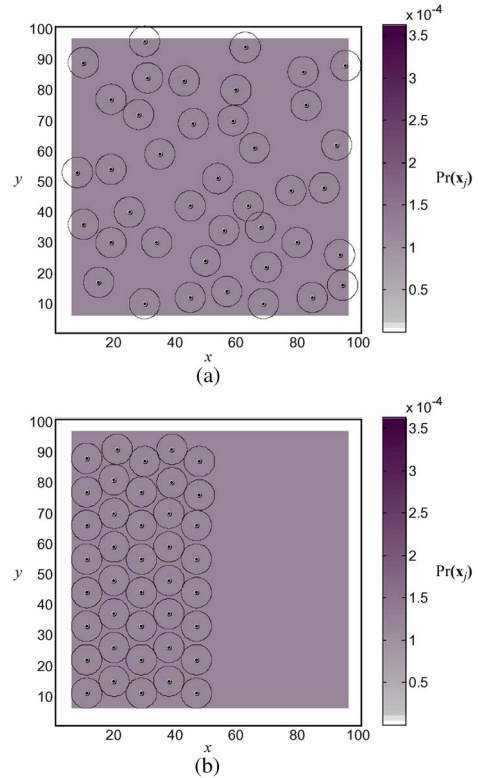


Fig. 10. Sensor networks obtained from a uniform pdf via (a) finite mixture sampling and (b) entropic sampling.

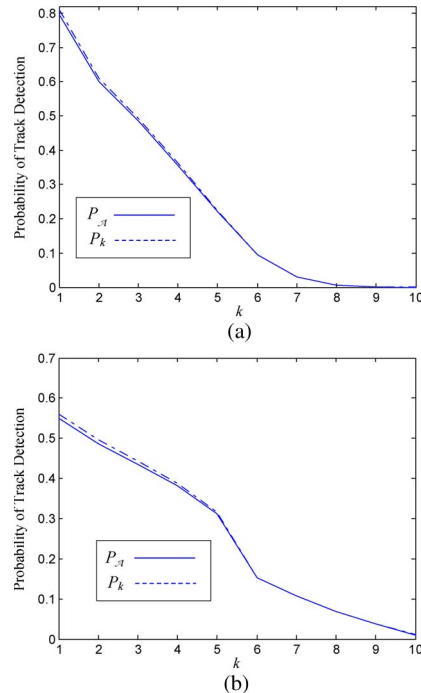


Fig. 11. Probability of track detection for the sensor networks obtained from a uniform pdf via (a) finite mixture sampling and (b) entropic sampling.

of track detection, P_A and P_k , are shown in Fig. 13. As in the previous examples, $P_A \approx P_k$, and the performance obtained via finite mixture sampling in Fig. 13(a) is higher than that obtained via entropic sampling in Fig. 13(b). However, entropic sampling typically leads to fewer intersections, i.e., higher

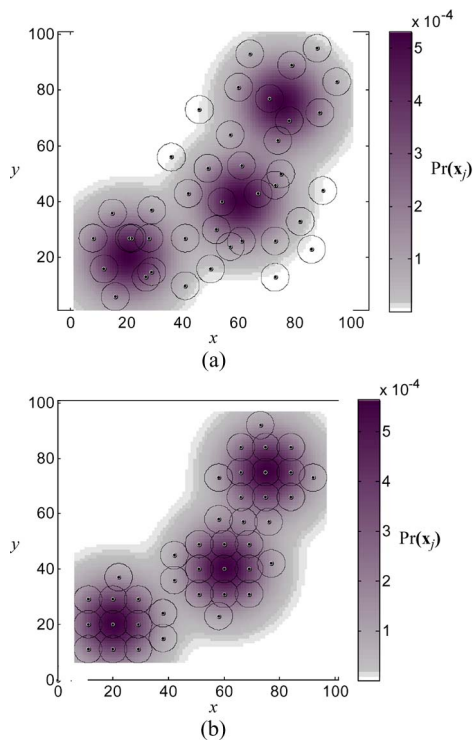


Fig. 12. Sensor networks obtained from a normal mixture pdf via (a) finite mixture sampling and (b) entropic sampling.

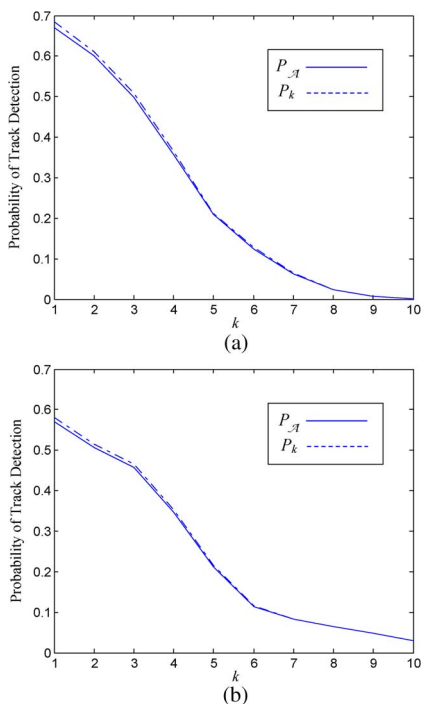


Fig. 13. Probability of track detection for the sensor networks obtained from a normal mixture pdf via (a) finite mixture sampling and (b) entropic sampling.

area coverage, than finite mixture sampling. Similar results are obtained for other pdfs but are omitted here for brevity.

Finally, the computation times required by P_A and P_k are compared in Table I for increasing values of k , and in Table II for increasing values of n . These simulations were conducted on a Pentium-4 CPU 3.06-GHz computer with 1-GB RAM.

TABLE I
COMPUTATION TIME REQUIRED BY P_A AND P_k WHEN $n = 40$ AND $r = 5$

k	1	2	3	4	5	6
P_A	0.249 s	0.187 s	0.174 s	0.173 s	0.173 s	0.172 s
P_k	120 s	115 s	114 s	114 s	114 s	115 s

TABLE II
COMPUTATION TIME REQUIRED BY P_A AND P_k WHEN $k = 2$ AND $r = 5$

n	3	5	20	40	60	80
P_A	0.105 s	0.0412 s	0.0898 s	0.175 s	0.265 s	0.359 s
P_k	93.2 s	91.1 s	92.0 s	91.3 s	91.9 s	92.5 s

The sensor networks are obtained via entropic sampling from the normal mixture density in (34). It can be seen from Tables I and II that the time to compute P_A by the geometric-transversal approach is less than 1% of the time required to compute P_k via direct evaluation. Therefore, it can be concluded that the geometric-transversal approach presented in this paper leads to performance functions that are computationally very efficient for both probabilistic and sampled (or deterministic) sensor networks.

VII. SUMMARY AND CONCLUSION

The quality of service of networks performing cooperative track detection, also referred to as track coverage, can be represented by the probability of obtaining multiple elementary detections over time along a target track. Distributed-search theory and geometric transversals have been used in the literature for representing the quality of service of these networks as a function of random and deterministic sensors' positions, respectively. Using Poisson flats, this paper extends the geometric-transversal approach, previously used to analyze the case of deterministic sensor positions and uniform target tracks, to the case of random sensor positions and nonuniform target tracks. A new performance function has been derived using a new approach that views the experiment of placing a Poisson flat in a Euclidean half-space as the experiment of placing points in a random interval in phase space. Through this approach, a new coverage factor has been defined in terms of the coverage cones generated by circles that are randomly placed in the ROI, representing the sensors' FOVs. The novel Poisson flat approach presented in this paper provides a unified framework for analyzing track coverage in both deterministic and probabilistic sensor networks. Furthermore, this paper proves that the distributed-search and geometric-transversal approaches previously presented in the literature are equivalent under the same problem formulation.

This paper also proves that these two approaches differ in the manner by which they integrate the joint sensor-target pdf over the space of all possible sensors' positions and target tracks. The theoretical results are demonstrated numerically in Section VI by simulating the deployment of probabilistic and sampled sensor networks. These simulations show that the Poisson flat approach presented in this paper leads to performance functions that are computationally very efficient for both types of networks and are equivalent to performance functions previously obtained via distributed search or direct evaluation.

REFERENCES

- [1] M. Xiang and J. Zhao, "On the performance of distributed Neyman–Pearson detection systems," *IEEE Trans. Syst., Man, Cybern. A, Syst., Humans*, vol. 31, no. 1, pp. 78–83, Jan. 2001.
- [2] T. A. Wettergren, R. L. Streit, and J. R. Short, "Tracking with distributed sets of proximity sensors using geometric invariants," *IEEE Trans. Aerosp. Electron. Syst.*, vol. 40, no. 4, pp. 1366–1374, Oct. 2004.
- [3] V. Isler, S. Khanna, and K. Daniilidis, "Sampling based sensor-network deployment," in *Proc. IEEE/RSJ Int. Conf. Intell. Robots Syst.*, 2004, vol. 100, pp. 1780–1785.
- [4] S. X. Yang and C. Luo, "A neural network approach to complete coverage path planning," *IEEE Trans. Syst., Man, Cybern. B, Cybern.*, vol. 34, no. 1, pp. 718–724, Feb. 2004.
- [5] N. Heo and P. K. Varshney, "Energy-efficient deployment of intelligent mobile sensor networks," *IEEE Trans. Syst., Man, Cybern. A, Syst., Humans*, vol. 35, no. 1, pp. 78–92, Jan. 2005.
- [6] V. Giordano, P. Ballal, F. Lewis, B. Turchiano, and J. Zhang, "Supervisory control of mobile sensor networks: Math formulation, simulation, and implementation," *IEEE Trans. Syst., Man, Cybern. B, Cybern.*, vol. 36, no. 4, pp. 806–819, Aug. 2006.
- [7] S. Ferrari, "Track coverage in sensor networks," in *Proc. Amer. Control Conf.*, 2006, pp. 1–10.
- [8] K. C. Baumgartner and S. Ferrari, "A geometric transversal approach to analyzing track coverage in sensor networks," *IEEE Trans. Comput.*, vol. 57, no. 8, pp. 1113–1128, Aug. 2008.
- [9] T. A. Wettergren, "Performance of search via track-before-detect for distributed sensor networks," *IEEE Trans. Aerosp. Electron. Syst.*, vol. 44, no. 1, pp. 314–325, Jan. 2008.
- [10] M. Ranasingha, M. Murthi, K. Premaratne, and X. Fan, "Transmission rate allocation in multisensor target tracking over a shared network," *IEEE Trans. Syst., Man, Cybern. B, Cybern.*, vol. 39, no. 2, pp. 348–362, Apr. 2009.
- [11] H. Cox, "Cumulative detection probabilities for a randomly moving source in a sparse field of sensors," in *Proc. Asilomar Conf.*, 1989, pp. 384–389.
- [12] J.-P. LeCadre and G. Souris, "Searching tracks," *IEEE Trans. Aerosp. Electron. Syst.*, vol. 36, no. 4, pp. 1149–1166, Oct. 2000.
- [13] B. Koopman, *Search and Screening: General Principles With Historical Applications*. New York: Pergamon, 1980.
- [14] P. Morse and G. Kimball, *Methods of Operations Research*. New York: Dover, 2003.
- [15] L. Stone, *Theory of Optimal Search*. New York: Academic, 1975.
- [16] D. Castañón, "Optimal search strategies in dynamic hypothesis testing," *IEEE Trans. Syst., Man, Cybern.*, vol. 25, no. 7, pp. 1130–1138, Jul. 1995.
- [17] G. V. Keuk, "Sequential track extraction," *IEEE Trans. Aerosp. Electron. Syst.*, vol. 34, no. 4, pp. 1135–1148, Oct. 1998.
- [18] R. V. Hogg, J. W. McKean, and A. T. Craig, *Introduction to Mathematical Statistics*. Upper Saddle River, NJ: Prentice-Hall, 2005.
- [19] Z. Kone, E. G. Rowe, and T. A. Wettergren, "Sensor repositioning to improve undersea sensor field coverage," in *Proc. OCEANS*, Sep. 2007, pp. 1–6.
- [20] E. Helly, "über mengen konvexer körper mit gemeinschaftlichen punkten," *Jahresbericht der Deutschen Mathematiker-Vereinigung*, vol. 32, pp. 175–176, 1923.
- [21] J. Goodman, R. Pollack, and R. Wenger, "Geometric transversal theory," in *New Trends in Discrete and Computational Geometry*, J. Pach, Ed. New York: Springer-Verlag, 1991, pp. 163–198.
- [22] D. P. Bertsekas, *Convex Analysis and Optimization*. Belmont, MA: Athena Scientific, 2003.
- [23] S. Skiena, "Generating k -subsets," in *Implementing Discrete Mathematics: Combinatorics and Graph Theory With Mathematica*. Reading, MA: Addison-Wesley, 1990, pp. 44–46.
- [24] J. Mecke, "Extremal properties of some geometric processes," *Acta Applicandae Mathematicae*, vol. 9, no. 1/2, pp. 61–69, Jan. 1987.
- [25] G. Matheron, *Random Sets and Integral Geometry*. New York: Wiley, 1975.
- [26] R. E. Miles, "A synopsis of Poisson flats in Euclidean spaces," in *Stochastic Geometry*, E. Harding and D. Kendall, Eds. New York: Wiley, 1974.
- [27] L. A. Santaló, *Integral Geometry and Geometric Probability*. London, U.K.: Addison-Wesley, 1976.
- [28] D. Stoyan, W. Kendall, and J. Mecke, *Stochastic Geometry*. New York: Wiley, 1987.
- [29] J. Mecke, "Random r -flats meeting a ball," *Archiv der Mathematik*, vol. 51, no. 4, pp. 378–384, Oct. 1988.
- [30] A. Papoulis and S. U. Pillai, *Probability, Random Variables, and Stochastic Processes*. New York: McGraw-Hill, 2002.
- [31] A. Poore and N. Rijavec, "A numerical study of some data association problems arising in multitarget tracking," *Comput. Optim. Appl.*, vol. 3, no. 1, pp. 27–57, 1994.
- [32] R. Popoli, "The sensor management imperative," in *Multitarget–Multisensor Tracking: Advanced Applications*, Y. Bar-Shalom, Ed. Norwood, MA: Artech House, 1992.
- [33] S. Deb, K. R. Pattipati, and Y. Bar-Shalom, "A multisensor–multitarget data association algorithm for heterogeneous sensors," *IEEE Trans. Aerosp. Electron. Syst.*, vol. 29, no. 2, pp. 560–568, Apr. 1993.
- [34] D. P. Bertsekas and J. N. Tsitsiklis, *Introduction to Probability*. Belmont, MA: Athena Scientific, 2002.
- [35] Mathworks, *Matlab*, Natick, MA, 2004, function: `quadl`. [Online]. Available: <http://www.mathworks.com>
- [36] R. Costa and T. A. Wettergren, "Assessing design tradeoffs in deploying undersea distributed sensor networks," in *Proc. OCEANS*, Vancouver, BC, Canada, Sep. 2007, pp. 1–5.
- [37] G. McLachlan, *Finite Mixture Models*. New York: Wiley-Interscience, 2000.
- [38] H. L. V. Trees, *Optimum Array Processing (Detection, Estimation, and Modulation Theory, Part IV)*, 1st ed. New York: Wiley-Interscience, 2002.
- [39] Mathworks, *Matlab*, Natick, MA, 2004, functions: `rand`, `mvnrnd`. [Online]. Available: <http://www.mathworks.com>

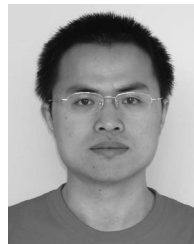


Silvia Ferrari (S'01–M'02–SM'08) received the B.S. degree from Embry–Riddle Aeronautical University, Daytona Beach, FL, and the M.A. and Ph.D. degrees from Princeton University, Princeton, NJ.

She is currently an Associate Professor of mechanical engineering and materials science with the Department of Mechanical Engineering and Materials Science, Duke University, Durham, NC, where she directs the Laboratory for Intelligent Systems and Controls (LISC). Her principal research interests include robust adaptive control of aircraft, learning

and approximate dynamic programming, and optimal control of mobile sensor networks.

Dr. Ferrari is a member of the American Society of Mechanical Engineers, The International Society for Optical Engineers, and the American Institute of Aeronautics and Astronautics. She was the recipient of the Office of Naval Research Young Investigator Award in 2004, the National Science Foundation CAREER Award in 2005, and the Presidential Early Career Award for Scientists and Engineers in 2006.



Guoxian Zhang (M'07) received the B.S. and M.S. degrees from Tsinghua University, Beijing, China, in 2003 and 2006, respectively. He is currently working toward the Ph.D. degree in mechanical engineering in the Department of Mechanical Engineering and Materials Science, Duke University, Durham, NC.

His research interests include sensor planning, data mining, multiagent systems, Bayesian statistics, and decision making under uncertainty.

Mr. Zhang is a member of the American Society of Mechanical Engineers.



Thomas A. Wettergren (A'95–M'98–SM'06) received the B.S. degree in electrical engineering and the Ph.D. degree in applied mathematics from Rensselaer Polytechnic Institute, Troy, NY.

In 1995, he joined the Naval Undersea Warfare Center (NUWC), Newport, RI, where he has served as a Research Scientist with the Torpedo Systems, Sonar Systems, and Undersea Combat Systems Departments. He is currently the U.S. Navy Senior Technologist for Operational and Information Science and a Senior Research Scientist at NUWC.

His current research interests are in the mathematical modeling, analysis, optimization, and control of undersea systems.

Dr. Wettergren is a member of the Society for Industrial and Applied Mathematics.